

Short Communication

Copper incorporated nanorod like mesoporous silica for one pot aerobic oxidative synthesis of pyridines

Suman Ray^a, Biplab Banerjee^b, Asim Bhaumik^{b,*}, Chhanda Mukhopadhyay^{a,**}^a Department of Chemistry, University of Calcutta, 92 APC Road, Kolkata 700009, India^b Department of Materials Science, Indian Association for the Cultivation of Science, Jadavpur, Kolkata 700032, India

ARTICLE INFO

Article history:

Received 19 May 2014

Received in revised form 26 August 2014

Accepted 1 September 2014

Available online 16 September 2014

Keywords:

Mesoporous silica nanorod

Copper incorporated silica

Redox catalyst

Pyridines

ABSTRACT

Copper incorporated nano-rod like mesoporous silica catalyst was synthesized, characterized by N₂ adsorption, HRTEM–EDX, XRD, AAS, XPS and TPD–NH₃ analyses and applied in the one-pot aerobic oxidative synthesis of highly substituted pyridines. Both the enhanced surface acidity of copper incorporated silica and the redox property were essential for pyridine synthesis. Standard leaching experiment proved that the reaction was heterogeneous.

© 2014 Elsevier B.V. All rights reserved.

1. Introduction

Oxidation of organic compounds represents an important approach towards the expansion of complex molecular structures. However, it remains a tremendous challenge to develop a quasi-nature catalyst for green and sustainable oxidation [1]. Oxidation by molecular oxygen as stoichiometric oxidant offers one of the most environmentally benign and ideal oxidation processes [2]. However, oxygen from air cannot be readily utilized for oxidation purposes. This is because organic molecules are in spin paired singlet state ($S = 0$) whereas oxygen molecule is in spin free triplet state ($S = 1$) and the reaction between singlet and triplet state is forbidden. All reactions of O₂ require initial activation from triplet to singlet state and thus the use of a catalyst becomes inevitable. The traditional catalysts for catalytic oxidation can be classified into the following categories: (a) supported precious metals [3,4]; (b) supported metal oxides and non-precious metals [5]; and (c) mixtures of metal oxides and precious metals [6]. Compared to precious metal/metal oxides, transition metal oxides are more abundant and less expensive [7]. However, the catalytic efficiency of bulk metal oxide is seriously restricted because of its low surface area. One way to circumvent this problem is to disperse the metal oxide particles onto supports with high surface area. If the metal oxide nanoparticles can be confined within a nanoporous host material, this may restrict the size to which the metal oxide nanoparticles can grow [7,8]. Mesoporous silicas have been considered as the most suitable hosts for the

stabilization of metal/metal oxide nanoparticles [9–11]. The nanoscale porosity of such supports may prevent the formation of large and catalytically inactive particles [12].

It has been noticed that silica and some of the support materials like alumina and zirconia exhibit a significant amount of surface acidity in the copper based catalysts [13]. Previously, silica supported copper has been utilized as an acid catalyst in the Biginelli, Mannich, different multicomponent reactions and catalytic transformation of benzyl alcohol [13–16]. Besides the modification of acidity, the presence of multivalent transition metal cations in the framework also creates isolated redox centers, which are suitable for their application as heterogeneous oxidation catalysts. Magnificent results have been achieved in transition metal incorporated silica catalyzed oxidation of benzyl alcohol, selective oxidation of cycloalkanes, oxidation of phenol and cyclohexanol, etc. [17,18].

In the present context, we have synthesized the copper incorporated nanorod like mesoporous silica catalyst and exploited both its surface acidity and the redox property in the one pot aerobic oxidative synthesis of pyridines using molecular O₂ as the stoichiometric oxidant (Scheme 1).

2. Experimental

2.1. Materials and instrumentation (see supporting information)

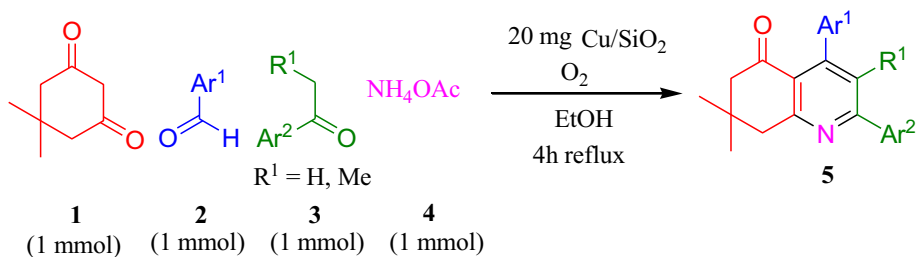
2.1.1. Preparation of copper incorporated silica nanorod

390 mL water and 400 mL MeOH were taken together in a 1 L open beaker fitted with a magnetic stirrer. Then 3.52 g CTAB was added at room temperature (30–35 °C) and stirred for 30 min. After a clear solution was obtained, tetraethylorthosilicate (TEOS) was added drop

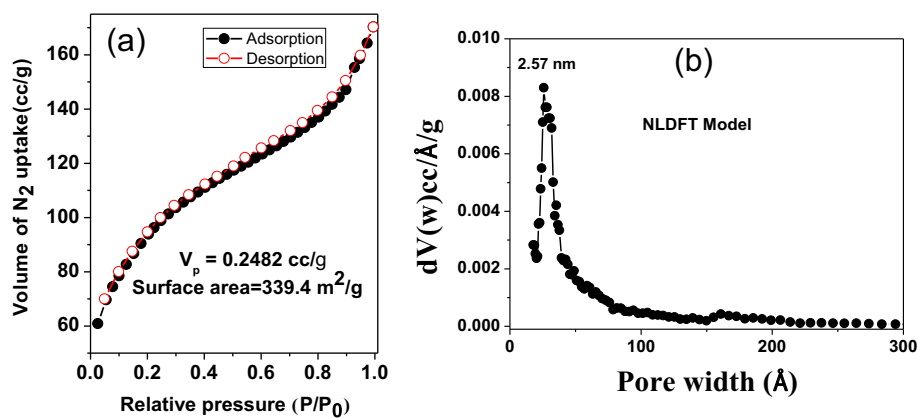
* Corresponding author.

** Corresponding author. Tel.: +91 33 23371104.

E-mail addresses: msab@iacs.res.in (A. Bhaumik), cmukhop@yahoo.co.in (C. Mukhopadhyay).

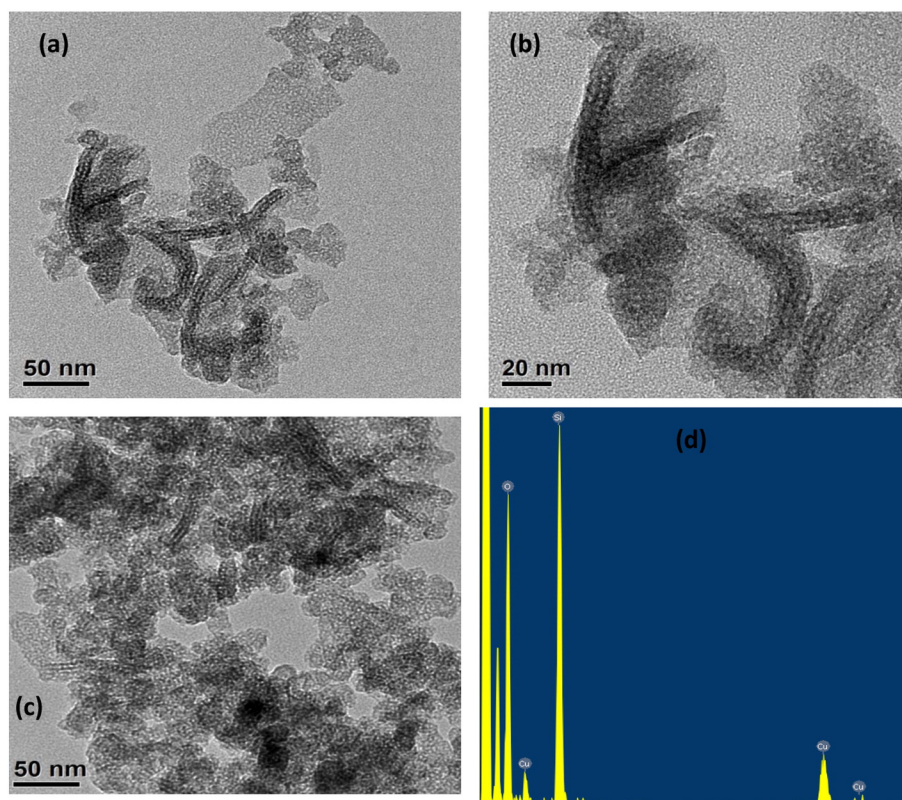


Scheme 1. Oxidative synthesis of pyridines.

Fig. 1. N₂ adsorption isotherm and pore size distribution of Cu/SiO₂.

wise from a dropping funnel under stirring condition. Next, 142.6 mg Cu(OAc)₂ was added and the stirring was continued for another 5 min. Then 10 mL 0.4 N NaOH solution was added drop wise taking

the time period of 1 h. The stirring was continued for the next 8 h at room temperature and then aged overnight (12–14 h) at room temperature. It was filtered, washed thoroughly with deionized

Fig. 2. (a–c) HRTEM images and (d) EDX spectrum Cu/SiO₂.

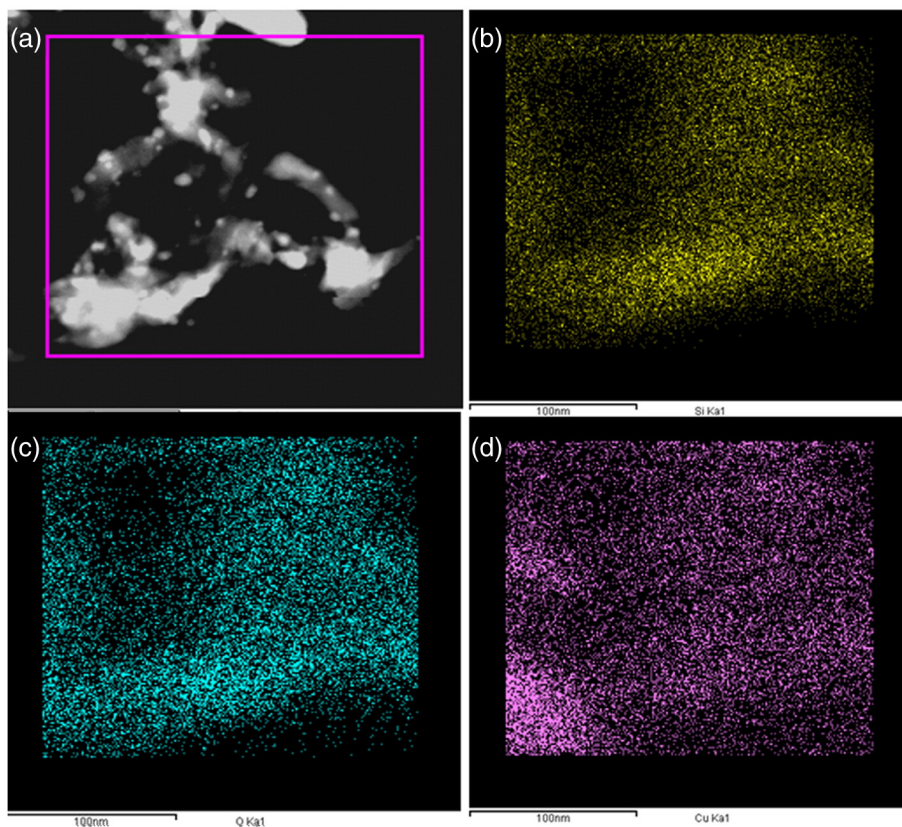


Fig. 3. Dark-field STEM image of a) Cu/SiO₂ and elemental mapping of b) Si, c) O, and d) Cu.

water and dried at 35–40 °C for 5 days. The dry powder was calcined at 550 °C for 6–8 h under static air.

2.1.2. Preparation of pyridines

The reactions were carried out in a three necked round-bottomed flask equipped with a flow of oxygen (10 mL/min). A mixture of ketone (1 mmol), 1,3-diketone (1 mmol), aldehyde (1 mmol) and ammonium acetate (1 mmol) in ethanol (4 mL) was refluxed for 4 h using 20 mg of the Cu/SiO₂ catalyst under a steady flow of O₂. After completion of the reaction, the ethanol was evaporated and the crude product was taken up in dichloromethane (5 mL) and filtered to separate the products as filtrate from the catalyst (residue). The solvent (dichloromethane) was evaporated in rotary evaporator and the crude product was further purified by silica gel column chromatography [10% EtOAc/90% petroleum ether (60–80 °C)].

All compounds were synthesized and characterized by IR, NMR and CHN analyses. Spectral data of the compounds are given in the supporting information.

3. Results and discussions

3.1. Characterization of catalyst

3.1.1. Nitrogen adsorption analysis

The isotherm shown in Fig. 1 (panel a) is a typical type IV isotherm with the presence of hysteresis loop, which indicates the presence of mesopores in the material [19]. The BET surface area calculated from this isotherm is found to be 339 m² g⁻¹. The estimated pore volume is 0.248 cc g⁻¹. Corresponding pore size distribution employing the non-local density functional theory (NLDFT) model is shown in panel b. Estimated pore dimension for

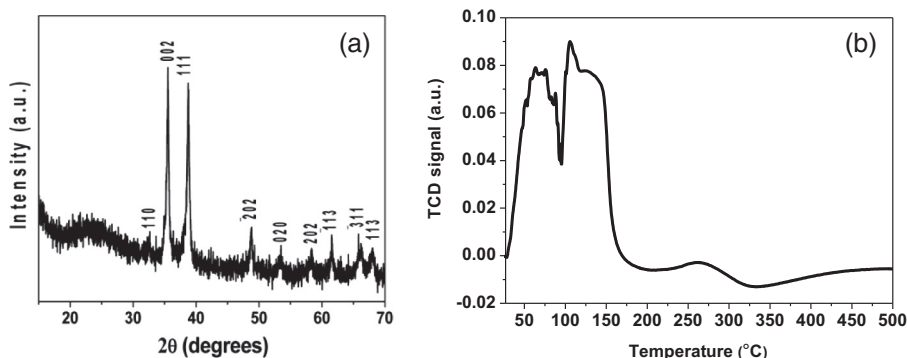


Fig. 4. (a) Powder XRD pattern and (b) TPD-NH₃ profile of Cu/SiO₂.

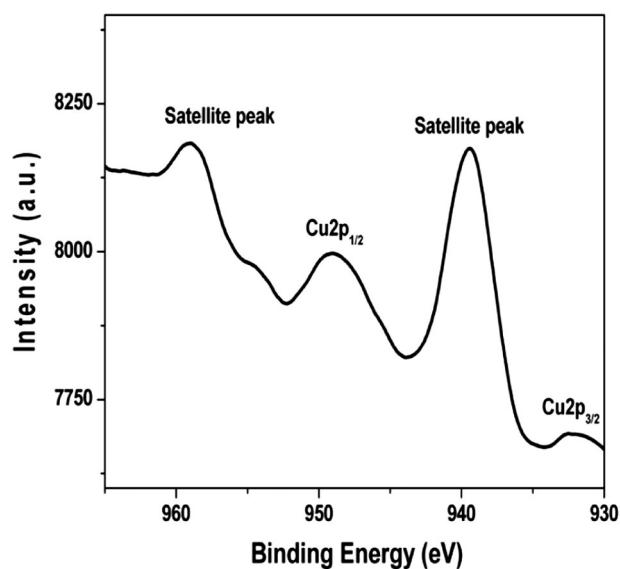


Fig. 5. XPS binding energy profile for Cu2p in Cu/SiO₂.

the sample is found to be 2.57 nm, which is in line with metal grafted mesoporous silica based materials synthesized by using CTAB as the template [20].

3.1.2. HRTEM–EDX analysis and EDX mapping

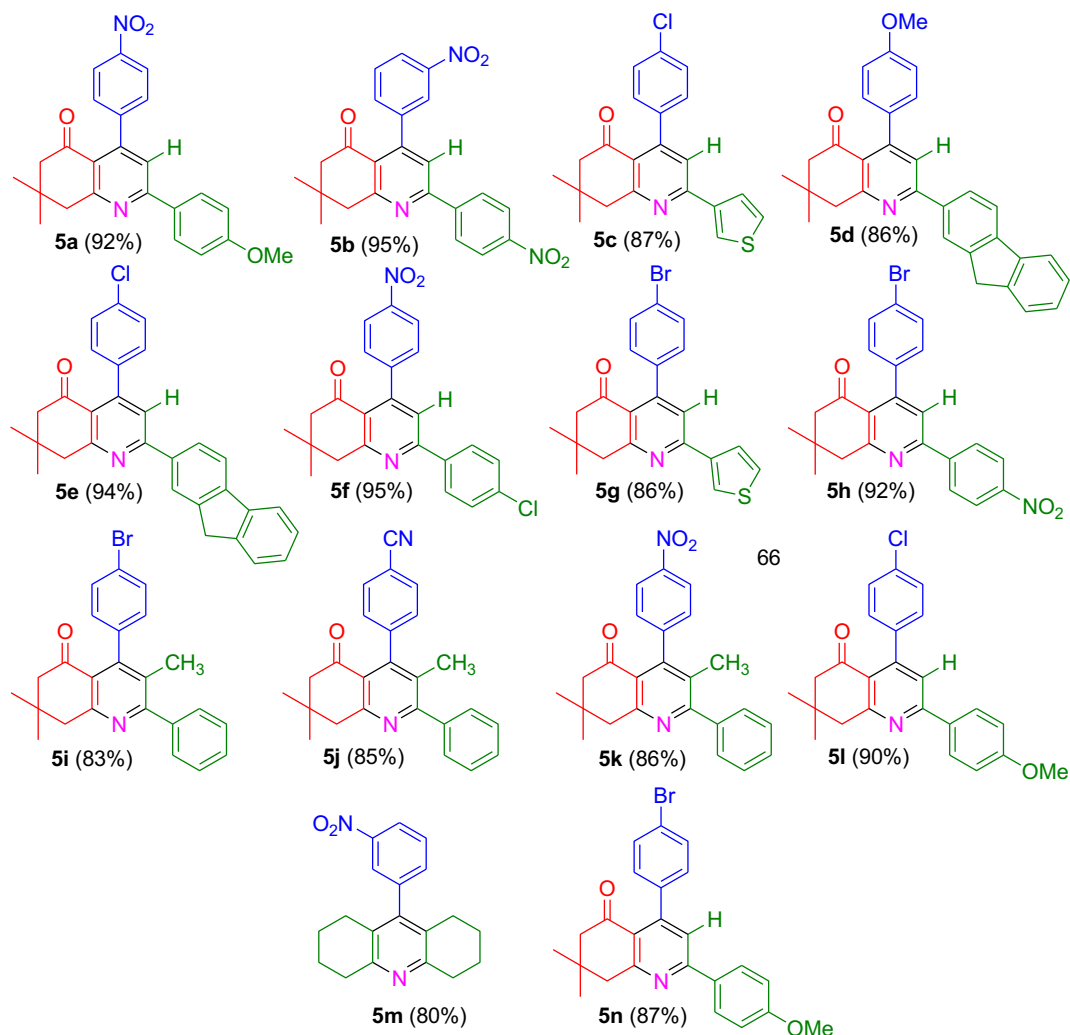
Representative TEM images show that the sample possesses porous nanorod like particle morphology. The dimension of the pores is 2–4 nm as seen throughout the specimen grid (Fig. 2, panels a–c). These data match well with the pore dimension obtained from N₂ sorption analysis. Chemical characterization of the material was carried out by EDX analysis. EDX analysis reveals that three elements, –O, Si and Cu, exist in the material (Fig. 2, panel d). Furthermore almost homogeneous distribution of copper on silica was confirmed by EDX-mapping (Fig. 3) [21].

3.1.3. Powder XRD

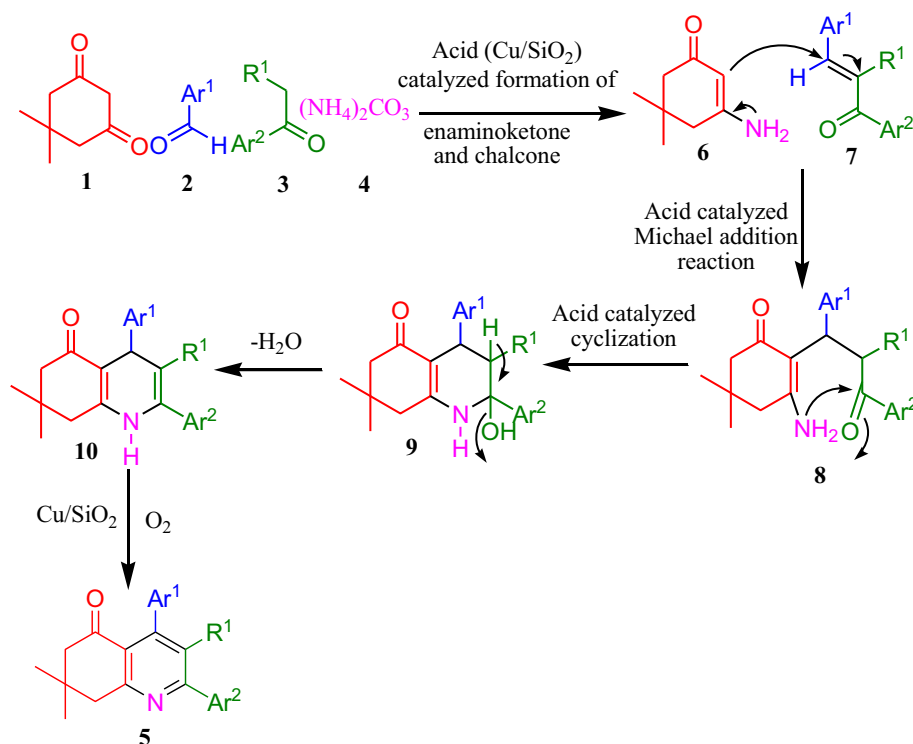
The formation of copper oxide within the silica matrix was confirmed by the powder XRD pattern of the material (Fig. 4, panel a). Several diffraction peaks can be indexed to the diffraction planes (110), (002), (111), ($\bar{2}02$), (020), (202), ($\bar{1}13$), ($\bar{3}11$), and (113) for CuO in the monoclinic phase [22].

3.1.4. TPD–NH₃ result

Surface acidity of the Cu/SiO₂ catalyst was determined by temperature programmed desorption of ammonia (TPD–NH₃). TPD–NH₃ profile (Fig. 4, panel b) indicates the presence of two major peaks centered at 68 °C and 107 °C, corresponding to two weak acid sites in the material. However, the total acidity calculated from this TPD profile is considerably high and amounts to 2.73 mmol g^{–1}. The high surface acidity could be responsible for high catalytic activity of this material [23].



Scheme 2. Structures of synthesized pyridines.



Scheme 3. Mechanism for the synthesis of pyridines.

3.1.5. AAS and XPS analysis

Atomic absorption spectroscopic analysis of the catalyst provides the accurate bulk content of Cu in the sample. Estimated Cu content was found to be 19.12 wt.%, suggesting very high loading of CuO in silica matrix. The XPS profile (Fig. 5) of the sample suggests the presence of $\text{Cu}2p_{3/2}$, $\text{Cu}2p_{1/2}$ and their corresponding satellite peaks, which are the characteristics of Cu(II) species bound at the silica surface [24].

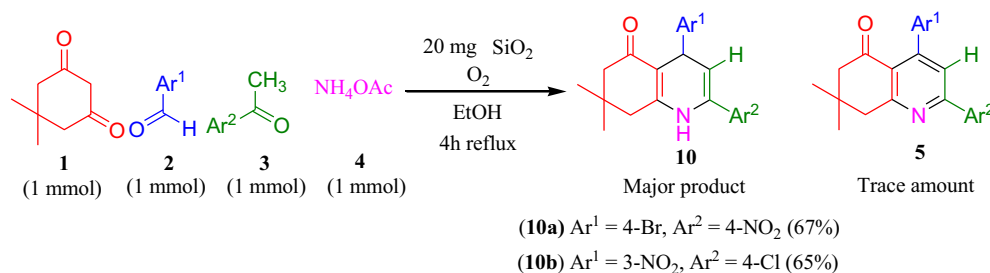
3.1.6. Catalysis

The reaction was first tried with different homogeneous acids like HCl, H_2SO_4 , HClO_4 , TFOH, PTS and AcOH in the presence of an additional oxidation catalyst (copper acetate) under a flow of oxygen (tables given in supporting information). Good to excellent conversion was achieved with these acids; however, they required repeated work-up, neutralization of strong acids and extensive chromatographic purification. Ultimately the isolated yields were not satisfactory. Different heterogeneous acid catalysts like TiO_2 , SiO_2 , and CeO_2 were also used. However, their acidity was not sufficient for good yields of the product. Compared to these catalysts copper incorporated silica (Cu/SiO_2) catalyst showed best isolated yield of pyridine. Therefore, Cu/SiO_2 was chosen both as an acid catalyst and as an oxidation catalyst for obtaining best yield of pyridine.

The acidity of Cu/SiO_2 was crucial for the cyclization but not sufficient to affect acid sensitive moieties like heteroaryl ketones and methoxy-substituted aryl aldehydes (Scheme 2). Sterically bulky 2-acetylfluorene reacted quantitatively under mild condition. Despite steric hindrance and ring tension, cyclic ketones also reacted smoothly. For precursors **2** and **3** bearing either electron-donating or electron-withdrawing substituents on the aromatic ring, all the reactions proceeded very efficiently to provide the corresponding pyridines.

3.1.7. Plausible mechanism

It is well known that introduction of copper within silica network produces enhanced surface acidity in comparison to pure silica [13]. The surface acidity of silica material is crucial for the condensation reactions producing 1,4-dihydropyridine and the redox property of the catalyst is responsible for oxidation of 1,4-dihydropyridine to pyridine. It is thought that the reaction proceeds via a cascade of condensation reactions (Scheme 3). At first, dimedone undergoes an acid catalyzed condensation with ammonia to form enaminoketone (**6**). Ketone also condenses with aldehyde to form chalcone (**7**). These two intermediates then undergo an acid catalyzed Michael addition type reaction to afford **8**. Subsequent acid catalyzed cyclization and dehydration give the 1,4-dihydropyridine (**10**). The cyclization of the intermediate **8** is initiated through protonation of its carbonyl oxygen



Scheme 4. Synthesis of 1,4-dihydropyridines (**10**).

by the Brønsted acidic sites of the Cu/SiO₂ catalyst or coordination with the Lewis acidic sites of Cu/SiO₂. The electrophilicity of the corresponding carbonyl carbon is thereby increased. Concomitant intramolecular nucleophilic attack by the nearby NH₂ group leads to cyclization product (**9**) which undergoes dehydration to give 1,4-dihydropyridine (**10**). This 1,4-dihydropyridine after being oxidized by molecular O₂ in the presence of the Cu/SiO₂ catalyst produces the target pyridine molecule (**5**).

In order to fully establish the role of the catalyst, the above reaction was carried out without any catalyst in ethanol under reflux. Practically no product was formed in that case. Again, 65–67% yield of 1,4-dihydropyridine was obtained along with trace amount pyridine when the reaction was carried out with pure silica without incorporation of Cu metal in the presence of oxygen (Scheme 4). The trace amount of pyridine probably resulted from the aerial oxidation of 1,4-dihydropyridine. Interestingly, when the reaction was repeated with the Cu/SiO₂ but in the argon atmosphere, no pyridine was formed but the 1,4-dihydropyridine was formed in excellent yield. Therefore, both the enhanced surface acidity and the redox behavior of the catalyst were necessary for the formation of pyridine in good yield.

3.1.8. Leaching test and recycling

In order to prove that the reaction was heterogeneous, a standard leaching experiment was conducted. A mixture of dimedone, 4-nitroacetophenone, 4-bromobenzaldehyde, and NH₄OAc in ethanol was allowed to react for 30 min under reflux in the presence of Cu/SiO₂. After 30 minute period the reaction mixture was filtered (hot). The filtered reaction mixture was then refluxed without the catalyst for the next 4 h; no further formation of the corresponding product was observed, indicating that no homogeneous catalyst was involved. XPS analysis of the filtrate showed that copper was not leached in the solution. The recycled catalyst could be used at least five times. Only a slight decrease in yield was due to loss of some amount of catalyst during filtration (recycling table given in supporting information).

4. Conclusion

Therefore, this protocol highlights the combined effects of both the enhanced surface acidity and the redox property of copper incorporated silica catalyst for the development of new eco-compatible strategy for heterocycle synthesis.

Acknowledgment

We acknowledge CSIR for fellowship (SR).

Appendix A. Supplementary data

Supplementary data to this article can be found online at <http://dx.doi.org/10.1016/j.catcom.2014.09.003>.

References

- [1] J.A. Jiang, C. Chen, J.G. Huang, H.W. Liu, S. Cao, Y. Fei Ji, *Green Chem.* 16 (2014) 1248–1254.
- [2] P. Hu, Q. Wang, Y. Yan, S. Zhang, B. Zhang, Z. Wang, *Org. Biomol. Chem.* 11 (2013) 4304–4307.
- [3] Z. Qu, S. Shen, D. Chen, Y. Wang, *J. Mol. Catal. A Chem.* 356 (2012) 171–177.
- [4] C.B. Zhang, H. He, K. Tanaka, *Appl. Catal. B Environ.* 65 (2006) 37–43.
- [5] X.F. Tang, Y.G. Li, X.M. Huang, Y.D. Xu, H.Q. Zhu, J.G. Wang, W.J. Shen, *Appl. Catal. B Environ.* 62 (2006) 265–273.
- [6] C.Y. Li, Y.N. Shen, M.L. Jia, S.S. Sheng, M.F. Adebajo, H.Y. Zhu, *Catal. Commun.* 9 (2008) 355–361.
- [7] J. Taghavi-moghaddam, G.P. Knowles, A.L. Chaffee, *J. Mol. Catal. A Chem.* 358 (2012) 79–88.
- [8] G. Laugel, J. Arichi, M. Molière, A. Kiennemann, F. Garin, B. Louis, *Catal. Today* 138 (2008) 38–42.
- [9] A. Martínez, C. López, F. Márquez, I. Díaz, *J. Catal.* 220 (2003) 486–499.
- [10] D. Yin, W. Li, W. Yang, H. Xiang, Y. Sun, B. Zhong, S. Peng, *Microporous Mesoporous Mater.* 47 (2001) 15–24.
- [11] Y. Ohtsuka, Y. Takahashi, M. Noguchi, T. Arai, S. Takasaki, N. Tsubouchi, Y. Wang, *Catal. Today* 89 (2004) 419–429.
- [12] A.Y. Khodakov, R. Bechara, A. Griboval-Constant, *Appl. Catal. A Gen.* 254 (2003) 273–288.
- [13] M. Dixita, M. Mishra, P.A. Joshi, D.O. Shah, *Procedia Eng.* 51 (2013) 467–472.
- [14] G. Kour, M. Gupta, S. Paul, R., V.K. Gupta, *J. Mol. Catal. A Chem.* 392 (2014) 260–269.
- [15] Z. Li, X. Ma, J. Liu, X. Feng, G. Tian, A. Zhu, *J. Mol. Catal. A Chem.* 272 (2007) 132–135.
- [16] S.M. Inamdar, V.K. More, S.K. Mandal, *Tetrahedron Lett.* 54 (2013) 579–583.
- [17] J. Andas, F. Adam, I. Ab. Rahman, *Appl. Surf. Sci.* (2014) <http://dx.doi.org/10.1016/j.apsusc.2014.07.118>.
- [18] S. Samanta, N.K. Mal, A. Bhaumik, *J. Mol. Catal. A Chem.* 236 (2005) 7–11.
- [19] M. Nandi, J. Mondal, K. Sarkar, Y. Yamauchi, A. Bhaumik, *Chem. Commun.* 47 (2011) 6677–6679.
- [20] D. Chandra, A. Bhaumik, *Ind. Eng. Chem. Res.* 45 (2006) 4879–4883.
- [21] A.K. Patra, A. Dutta, A. Bhaumik, *Chem. Eur. J.* 19 (2013) 12388–12395.
- [22] D.P. Volanti, D. Keyson, L.S. Cavalcante, A.Z. Simões, M.R. Joya, E. Longo, J.A. Varela, P.S. Pizani, A.G. Souza, *J. Alloys Compd.* 459 (2008) 537–542.
- [23] S.K. Das, M.K. Bhunia, A.K. Sinha, A. Bhaumik, *ACS Catal.* 1 (2011) 493–501.
- [24] J.P. Espinos, J. Morales, A. Barranco, A. Caballero, J.P. Holgado, A.R. Gonzalez-Elipe, *J. Phys. Chem. B* 106 (2002) 6921–6929.